

JANUSZ KRUCZKOWSKI\*, JERZY KRAWCZYK\*<sup>#</sup>, PIOTR OSTROGÓRSKI\***LABORATORY INVESTIGATIONS OF STATIONARY METHANE ANEMOMETER****BADANIA LABORATORYJNE METANOANEMOMETRU STACJONARNEGO**

This paper presents a new stationary device that can perform simultaneous measurements of air flow velocity and methane concentration in a mine heading (stationary methane anemometer). The test station is designed to use the instrument to test the effect of various parameters on the air-methane stream. The air velocities and methane concentrations were fed to the measuring area via an injector and recorded. The results present numerical simulations of flow phenomena that occurred during measurement experiments.

**Keywords:** ventilation of mines, mining aerology, methane concentration, anemometer, methane anemometer, CFD analysis

W artykule zaprezentowano nowe, stacjonarne urządzenie do jednoczesnego pomiaru prędkości przepływu powietrza i stężenia metanu w wyrobisku kopalni (metanoanemometr stacjonarny). Przedstawiono stanowisko badawcze pozwalające na przeprowadzenie eksperymentów pomiarowych polegających na oddziaływaniu na przyrząd strugą mieszaniny powietrzno-metanowej o zmiennych parametrach. Zarejestrowano przebiegi prędkości i stężenia metanu podawanego do obszaru pomiarowego za pomocą iniektora. Pokazano wyniki symulacji numerycznej zjawisk przepływowych zachodzących podczas eksperymentów pomiarowych.

**Słowa kluczowe:** wentylacja kopalń, aerologia górnicza, stężenie metanu, anemometr, metanoanemometr, analiza CFD

## 1. Introduction

An essential problem in the metrology of underground mine ventilation networks is the measurement of the methane volume stream. Despite the adoption of a few measurement procedures in previous years, only recently has research been undertaken aimed at the verification of their

\* THE STRATA MECHANICS RESEARCH INSTITUTE OF THE POLISH ACADEMY OF SCIENCES, UL. REYMONTA 27, 30-059 KRAKÓW, POLAND

<sup>#</sup> Corresponding author: [krawczyk@img-pan.krakow.pl](mailto:krawczyk@img-pan.krakow.pl)

accuracy and feasibility of use based on flow and environmental conditions, The factors which may impact the accuracy of measurement results include the separation of air volume stream measurements from average methane concentration measurements in the cross-section. Research aimed at the construction of measurement devices in which both parameters are measured simultaneously (Janus et al., 2013; Kruczkowski & Ostrogórski, 2013) is being carried out in the IMG PAN (Eng. *The Strata Mechanics Research Institute of the Polish Academy of Sciences*). The first instrument where simultaneous measurements were determined was the portable methane anemometer denoted as SOM 2303 (Kruczkowski & Ostrogórski, 2015). The sensors of air flow velocity and methane concentration used in the measurement experiment recorded quasi-point-by-point measurements of both values at the same time. After entering the information about the size of the heading cross-section, the instrument measures methane volume stream by the continuous traverse method. At present, after having obtained required certificates, the methane anemometer was deployed for use in underground coal mines. The experience gained during its construction and the positive opinions on the increase in the quality and accuracy of measurements were the basis for undertaking research on a corresponding solution in a stationary form. An additional factor justifying the decision was to attempt to control air flow directly, very close to the methane sensor. This would enable observation of any possible disruptions to operating conditions.

As opposed to a hand-held methane anemometer, a stationary instrument needs to perform additional activities in order to measure the methane volume stream. The requirements are the same as for the hand-held methane anemometer intended for the measurement of the air volume stream (Wasilewski et al., 2015). The correction coefficient for the measured local velocity in relation to the average velocity at the place of installation should be determined. The measured local methane concentration can be assumed to represent the average value provided that methane is thoroughly mixed in the heading cross-section. This paper presents the results of the measurement laboratory experiment concerning the effect of the methane stream on the concentration sensor of the stationary methane anemometer under the flow conditions where a lack of mixing methane with air may be suspected. In addition to the measurement experiments, numerical simulations of the phenomena occurring during the flows generated on the test stations were also carried out.

## 2. Methane anemometer description

The stationary methane anemometer shown in photo (Fig. 1) is the device which performs simultaneous measurement of air flow velocity in a mine heading and the concentration of methane contained in this air flow. The concept of the project was presented in the previous publications (Kruczkowski, 2013b; Janus et al., 2013; Kruczkowski & Ostrogórski, 2013). The measuring device was built because there was no other equivalent among the meters of the physical parameters of the mine atmosphere which could perform the desired measurements.

The instrument shown in the photo above consists of a vane anemometer velocity sensor and a methane concentration pellistor sensor; both sensors were placed in a common tube shield. The methane sensor is located in the upper part of the shield from the side of the expected air inflow. Between the methane concentration sensor and the velocity sensor a palisade of three bars protecting the vane against mechanical damage.

The same palisade is behind the sensor. Placing the methane concentration sensor in front of the palisade allows calibration using the standard procedure for stationary methane anemometers. Above the shield of the sensor is a chamber with electric circuits with communication terminals.

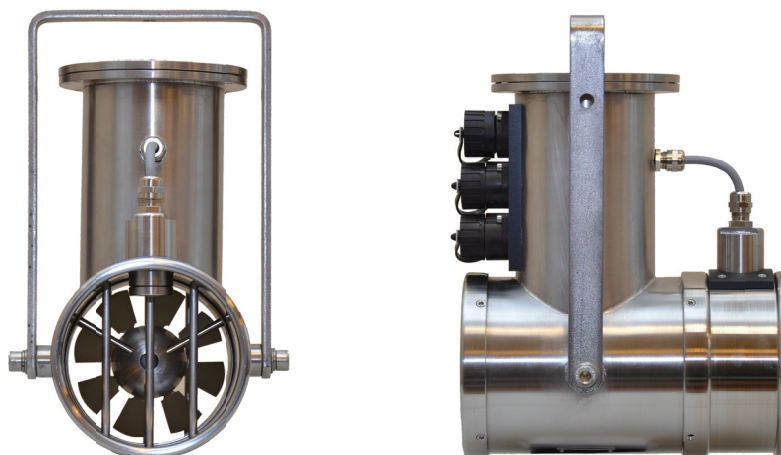


Fig. 1. Stationary methane anemometer

The methane anemometer was fitted with three terminals which connect to a transmission-power supply line, data monitor, and alarm signals, as well as two-state control circuits. The instrument is designed for interaction with the most modern generation of digital telemetry systems due to the type of information generated. Apart from the main sensors, an outer element measuring temperature was built-in into the lid that closes the chamber of the electronic circuits. The thermometer's measuring range records high temperatures which can occur in catastrophic conditions. The structure of the methane anemometer was designed with such situations in mind, and considerably exceeds the requirements for regular mining measuring instruments. The electronic system also records data in the "Black Box" technology after the external power supply-transmission lines are broken.

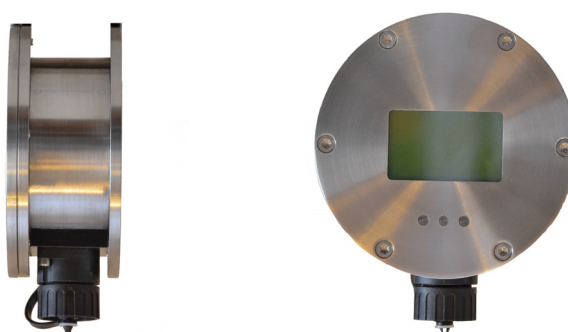


Fig. 2. The monitor of the stationary methane anemometer

The monitor shown in photo (Fig. 2) is an additional equipment element of the methane anemometer and allows direct access to data from the distance of up to a few hundred meters. The monitor functions as an optical alarm signaling device and also calibrates the methane sensor

in underground conditions. Most elements of both devices are made of high-grade acid resistant steel guarantying resistance to the aggressive mine environment.

The range of measurement of flow velocity is  $\pm (0.16$  up to  $12$  m/s) and the range of the measurement of methane concentration is  $0$  up to  $100\%$ . The frequency of measurement is  $1$  Hz.

### 3. Test station

The structure of the test station was dictated by the necessity to check the operation of the new device and to make the observations of the methane concentration sensor, depending on the how the air-methane mixture enters the system. An attempt to create a methane path in the air stream with adjustable flow velocity was undertaken. It was appropriate to make the assumption that methane will not be completely mixed with air, and by this, the adverse phenomena could be observed when the instrument is possibly used as a stationary meter of the methane volume stream. However, in most mine headings a homogenous distribution of the methane concentration field in the heading cross-section can be expected, the presence of other distribution patterns cannot be excluded (Skotniczny, 2014; Kruczkowski, 2013a).

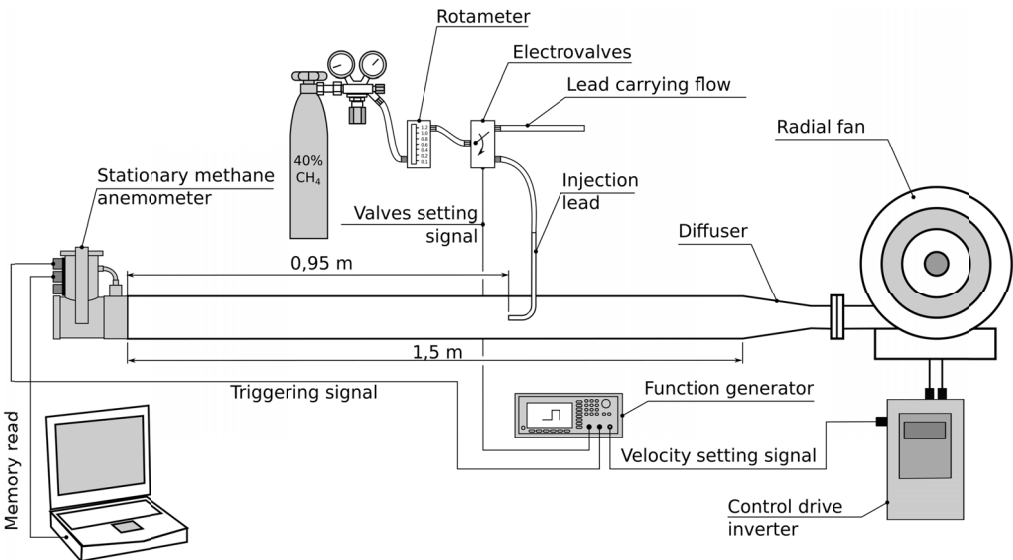


Fig. 3. Test station for the investigation of the stationary methane anemometer

The test station shown in Fig. 3 consists of a section of the pipeline  $1.5$  m long with an inner diameter of  $0.11$  m. The pipeline was connected with the radial fan by means of the diffuser with an inlet diameter of  $0.05$  m. The rotational speed of the fan was adjusted by the inverter. The tested methane anemometer was installed at the end of the pipeline. An air-methane mixture of  $40.36\%$  is fed to the inside of the pipeline by the injector made of the pipe bent at the angle of  $90^\circ$ . The inner diameter of the pipe is  $0.008$  m. The time of feeding mixture was set by means

of the unit of the coil electrovalves. The output of the mixture was controlled by the rotameter installed between the pressure reducer and the coil valves. The distance between the injector outlet and the methane anemometer inlet is 0.95 m. The device controlling the experiments was an arbitrary generator initiating the operation of the methane anemometer, controlling the coil valves, and the fan inverter. The station measured out the time of mixture feeding, setting the mixture stream quantity, and the smooth adjustment of the flow velocity inside the pipeline. There was also a possibility of the synchronisation of the recording time and the opening of the electrovalves. The measurement data were gathered in the methane anemometer memory and then analysed by the computer.

#### 4. Results of the investigations

The investigation of the stationary methane anemometer involved injecting the inlet of the instrument measurement section with an air stream of known and controlled velocity. Known concentrations of methane and air stream volume were fed to the air stream. The standard measurement frequency of 1 Hz was increased to 10 Hz. This frequency was sufficient for the methane concentration sensor. The pellistor sensor contains its own electronic circuit which can give responses with required frequency, but the limitation in the A/C converter line of the pellistor bridges results in a change of the analogue signal limited to 5 Hz. Hence, in the presented charts the characteristic serration can be seen. However, this signal has no substantial importance for the discussion of the paper.

After a series of trial measurements, it was established that the volume of the air-methane mixture stream fed to the pipeline will be constant for all the experiments and its value will be 1.2 l/min. This flow rate allowed measurement of the methane concentration over various time points and air stream velocities. The velocity of the outflow of the established mixture stream from the injection pipe was 0.4 m/s. Figs. 4-6 present the concentrations recorded by the methane sensor under constant methane concentration but varying air stream velocities. The change in methane concentration with time is recorded by the methane sensor.

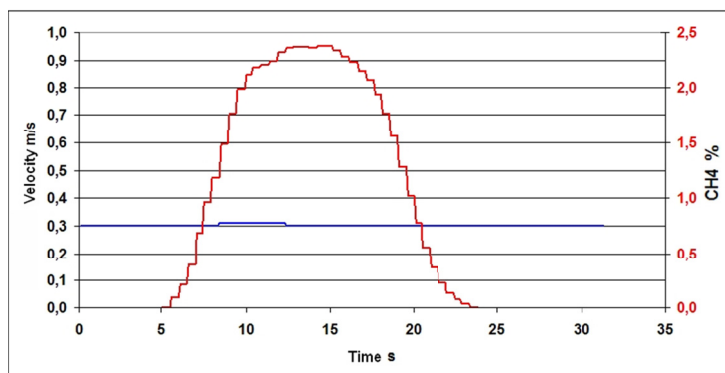


Fig. 4. Recording of the delay time of the methane propagation from the injector outlet to the methane concentration sensor.

Duration of mixture inflow = 10 s. Air stream velocity = 0.3 m/s

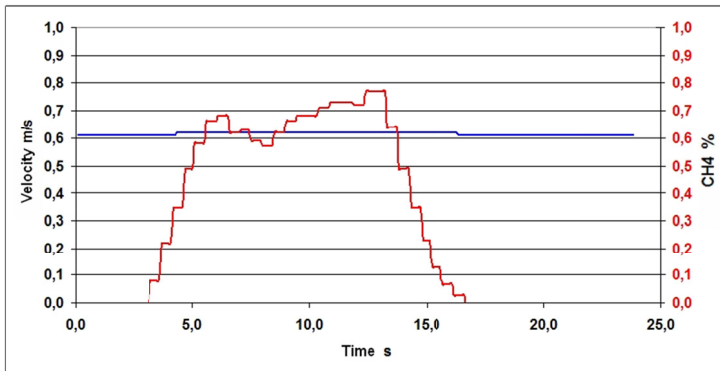


Fig. 5. Recording of the delay time of the methane propagation from the injector outlet to the methane concentration sensor.

Duration of mixture inflow = 10 s. Air stream velocity = 0.6 m/s

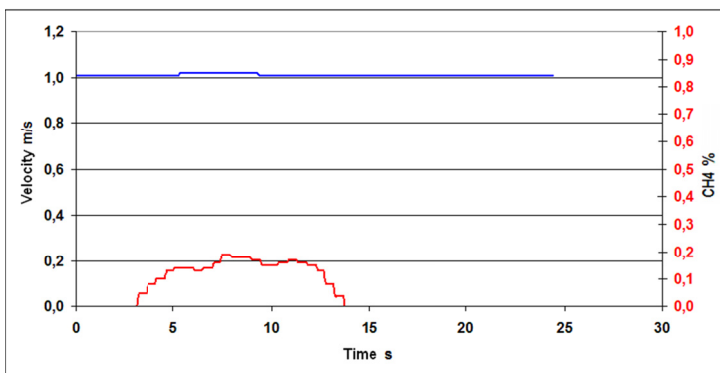


Fig. 6. Recording of the delay time of methane propagation from the injector outlet to the methane concentration sensor.

Duration of mixture inflow = 10 s. Air stream velocity = 1.0 m/s

For the case shown in Fig. 4, with the stream velocity of 0.3 m/s, the reaction occurred after 5.1 s. The maximum recorded methane concentration was 2.38%. With the stream velocity of 0.6 m/s, the reaction occurred after 3.2 s and the maximum recorded methane concentration was 0.77%. And finally, with the stream velocity of 1.0 m/s, the reaction occurred after 3.1 s and the maximum recorded methane concentration was 0.18%. In each case, the reaction time was greater than the time needed for the displacement of the air stream from the injector outlet to the sensor. Also, lower methane concentrations were recorded, as the velocity increased. This proves that the streams did not intermingle within this section and that a methane stream was formed which partially bypassed the concentration sensor.

Figs. 7, 8, and 9 present the results of the mixture pulse propagation, over different durations. The aim was to observe how the methane concentration is being formed in the flow condition similar to steady state. It can be noted that with the increase in the air stream velocity the sensor

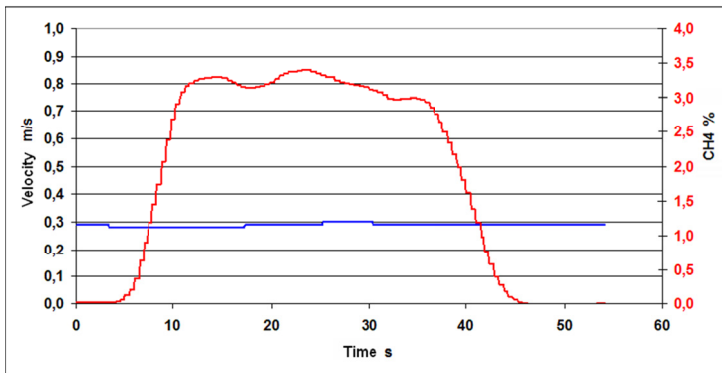


Fig. 7. Recording of the methane concentration fluctuation during the air-methane mixture propagation.  
Duration of the mixture inflow = 30 s. Air stream velocity = 0.3 m/s

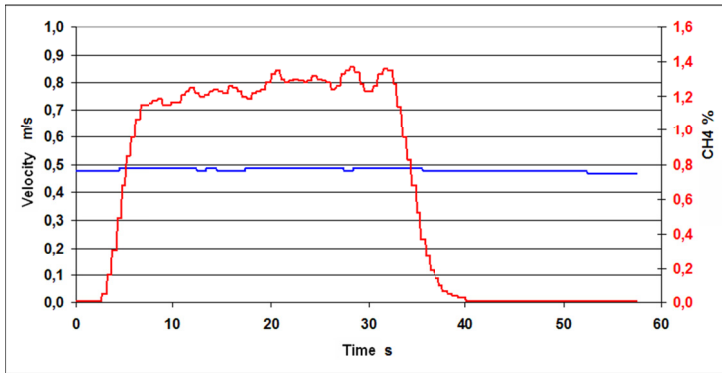


Fig. 8. Recording of the methane concentration fluctuations during the air-methane mixture propagation.  
Duration of the mixture inflow = 30 s. Air stream velocity = 0.5 m/s.

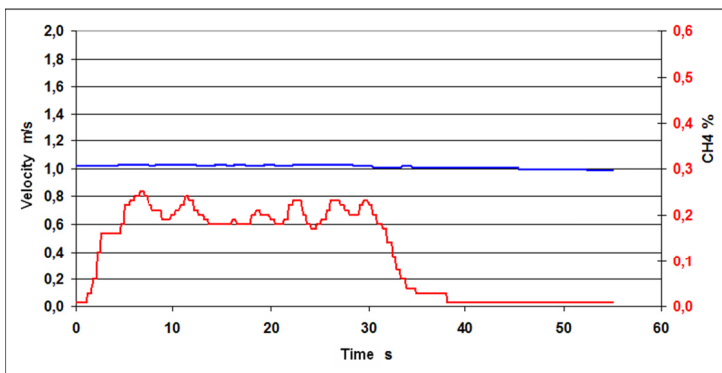


Fig. 9. Recording of the methane concentration fluctuations propagation during air-methane propagation.  
Duration of the mixture inflow = 30 s. Air stream velocity = 1.0 m/s

records lower methane concentrations. Also, the pulse duration becomes shorter. The measured concentration values prove that no full intermingle of air occurred after the mixture is fed. The calculations show that the methane concentration should be 0.3% for the ideal intermingle. The measured values are much higher. This confirms the hypothesis that a methane path was formed between the end of the injector and the inlet surface of the methane sensor measurement chamber. With the increase in the air stream velocity the fluctuations of the methane concentrations also increases.

The investigation aimed to determine the mixture pulse feeding time needed to settle the methane concentration. As shown in Fig. 7, for the 0.3 m/s flow velocity, the methane concentration being measured settles for the mixture feeding times longer than 7 s. After this time the increase in pulse duration does not cause any changes in the concentration being measured, and the high fluctuations of its values can be seen.

In addition, there were investigations into changes of the methane concentration sensor during sinusoidal changes of flow velocity. To this end, the inverter was programmed so that the frequency of the velocity changes was 0.1 Hz. The amplitude of the velocity changes was 0.18 m/s. The changes of the methane concentration are shown in Fig. 9. In Fig. 10 the analogous recording for the frequency of 0.2 Hz is presented. The increase in the frequency of air stream velocity changes caused a reduction in the amplitude of concentrations being recorded and shortened the time of methane removal.

Fig. 11 shows the delay which occurs between the velocity changes being recorded by the anemometric sensor and methane concentration changes. The reduction in the velocity causes the increase in the concentration with a certain delay. The shift between both signals results from the different dynamic properties of the vane sensor and the methane sensor.

## 5. Numerical simulations. Model and assumptions

The geometry of the test station and the methane anemometer was generated based on CAD software imported to the Gambit grid generator. The geometry of the area is shown in the figure

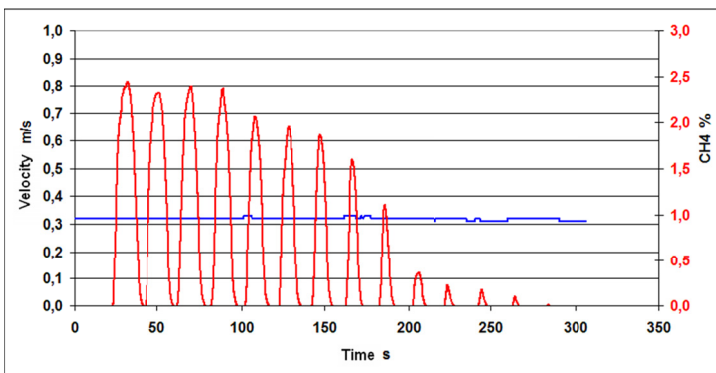


Fig. 10. Propagation of the methane concentration for the flow velocity 0.3 m/s.  
Duration of pulses 9, 8, 7, 6, 5, 4, 3, 2, 1, 0.8, 0.6, 0.4, 0.2 s, respectively.  
The frequency of mixture feeding is 0.05 Hz



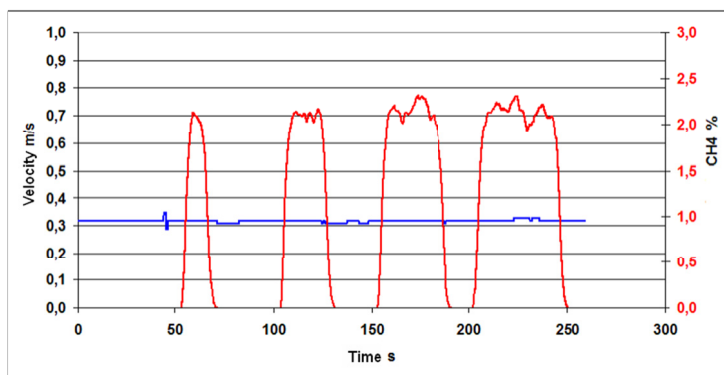


Fig. 11. The propagation of the methane concentration for the flow velocity 0.3 m/s. Durations of pulses 10, 20, 30 and 40 s, respectively. The frequency of mixture feeding is 0.017 Hz

where the positions of the virtual methane concentration sensors were marked. It was assumed that a vane of the anemometer is in motion and affects the velocity field to a negligible extent. A non-stationary, three-dimensional flow of the air-methane mixture was considered with the displacement taken into account. Flat velocity profiles were assumed on the diffuser inlet and the outlet of the pipe feeding the air-methane mixture. The preliminary calculations were carried out for the  $k-\epsilon$  turbulence model, whereas the target calculations were carried out by the  $k-\omega$  SST model. The Fluent (ANSYS, 2015) software was used for the calculations.

## 6. Calculations of the initial state

The initial state, before the mixture was fed, was generated by carrying out the calculation for 5 seconds. It was assumed that the pipe is filled with the air-methane mixture. Preliminary calculations were carried out until the stationary concentration field was obtained.

The diffuser is located at the inlet of the model. The angle of the diffuser is so large that the flow is torn away and the turbulence generation increases. This is proved by the rotation contours. The difference between the cross-sections of the diffuser inlet and outlet is about 4, and this causes a quadruple drop of the average velocity in the pipe of the station. The pipe section from the diffuser to the anemometer inlet is too short to create a developed velocity profile. At the distance of 0.95 m before the methane anemometer there is a bent pipe for feeding the methane and air mixture, which constitutes a local flow disturbance and extends about 0.5 m. At the instrument inlet, there is a slight cross-section narrowing causing only a small increase in the velocity. On the inlet of the anemometric sensor, there is a bar palisade protecting the sensor. The bars generate a rotary path. Further, there is a hemisphere-shaped cup suspended on three bars. The cap narrows the cross-section causing an increase in the velocity in the area of the inflow on the vane. The second cap is practically located in the aerodynamic shadow generated by the first one. The cap supports constitute another source of flow disturbance. A similar impact on the flow was the second palisade at the sensor outlet. It was assumed that the injection pipe is filled with the air-methane mixture. Through the outlet cross-section methane diffuses to the air flowing in the pipeline and is swept towards the outlet. On the way to the outlet, the methane is

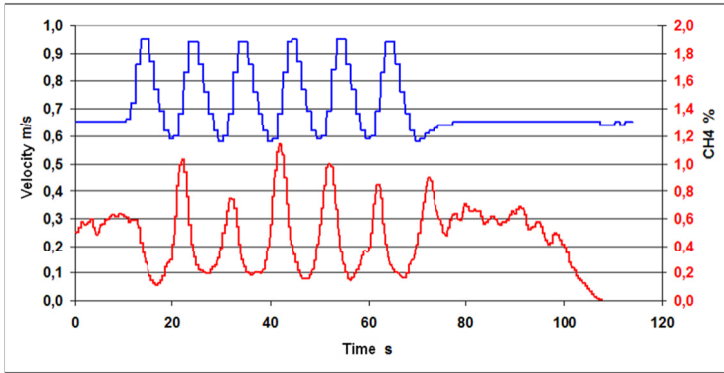


Fig. 12. The changes in the methane concentration caused by the changes in the air stream velocity. The initial flow velocity was 0.65 m/s and the frequency 0.1 Hz

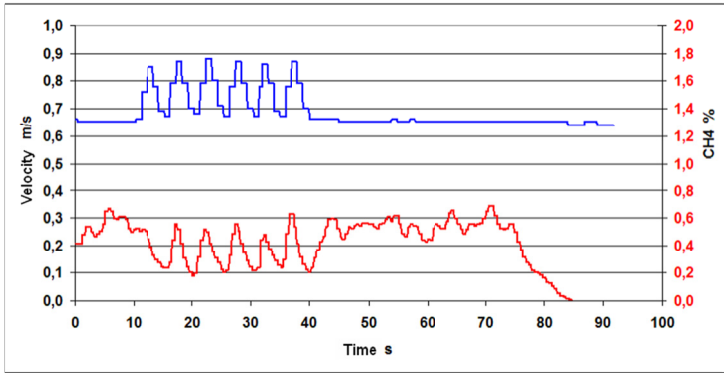


Fig. 13. The changes in the methane concentrations caused by the changes in the air stream velocity. The initial flow velocity was 0.65 m/s and the frequency 0.1 Hz

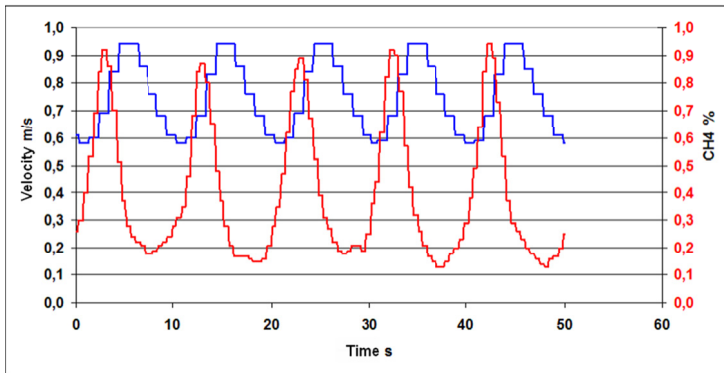


Fig. 14. The changes in the methane concentration caused by the changes in the air stream velocity. The initial flow velocity was 0.6 m/s and the frequency 0.1 Hz

gradually diluted due to the turbulent diffusion. The displacement causes a slight deviation of the concentration field upwards. In this case, the simulation assessed not only the initial velocity field but also the field of concentrations. The methane concentration field constituted a marker useful to determine if the expected initial state was achieved. That was indicated by the steady point sensor readings and also by the fact that the gas stream has reached the station outlet, Figs. 12-14.

## 7. Response to the discrete methane inflow

In the next stage, a discrete increase in the methane inflow velocity up to 0.4 m/s was set, which corresponds to the  $0.2E-3 \text{ m}^3/\text{s}$  stream. It was assumed that opening the coil valve causes the increase in the methane outflow velocity at 0.6 second, i.e. during six-time steps of the simulation. The course of the increase in velocity is presented in Table 1.

The volume stream at the diffuser inlet was  $0.00255 \text{ m}^3/\text{s}$  which corresponds to  $0.0029 \text{ kg/s}$ . The methane mixture stream was  $1.68E-05 \text{ kg/s}$  which, at the mass share of  $0.279 \text{ kg/kg}$ , gives  $0.47E-05 \text{ kg/s}$  of pure methane. When ideal mixing of the streams occurs the mass share is  $1.61E-03 \text{ kg/kg}$  or  $0.28\%$  of the volume.

The calculation of the methane propagation for a constant inflow was continued for 6 s recording the intermediate states every 0.1 second. The average methane concentration at the inflow to the sensor measuring chamber (inlet filter) was recorded. The concentrations were monitored pointwise for the points in the station axis (methane anemometer inlet 0.1, 0.3, 0.5, 0.7, and 0.9 m before inlet) and at one point close to the methane sensor. Also, the following methane concentration values were monitored: average, maximum and minimum, for the cross-sections of 0.3 and 1 m before the sensor in the sensor cross-section, and in the methane anemometer inlet and outlet cross-section.

TABLE 1

Increase in the methane inflow velocity

Time s	Velocity m/s	Stream l/min	CH <sub>4</sub> stream l/min
5	0	0	0
5.01	0.1	0.268359	0.10788
5.02	0.3	0.805078	0.323641
5.03	0.35	0.939258	0.377582
5.04	0.375	1.006348	0.404552
5.05	0.3875	1.039892	0.418037
5.06	0.4	1.073437	0.431522

The calculation results are presented in the form of the charts of the concentration changes with time (Fig. 16). In addition, the distribution of the concentrations with time for both vertical and horizontal cross-sections along the station axis are shown.

After opening the valve, the stream moves with the velocity only slightly higher than the velocity of the ambient air. The displacement forces convect the stream upwards. Before the methane anemometer inlet, the stream reaches the upper wall of the pipe and sticks to it. The sensor housing is lipped by the stream and the sensor filter surface (inlet to the measuring chamber) is in the centre of the stream where the maximum concentrations occur. The simulated average

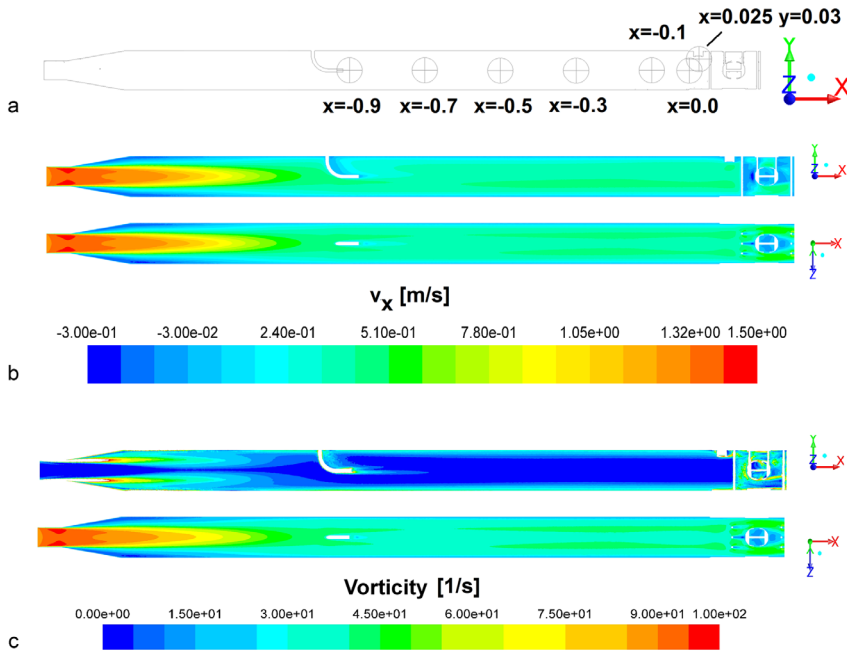


Fig. 15. The location of the virtual concentration sensors and the initial flow state. a) the location of the sensors in the vertical cross-section of the station; b) velocity field – component parallel to the axis; c) vorticity distribution within the range of 0 up to 100 1/s

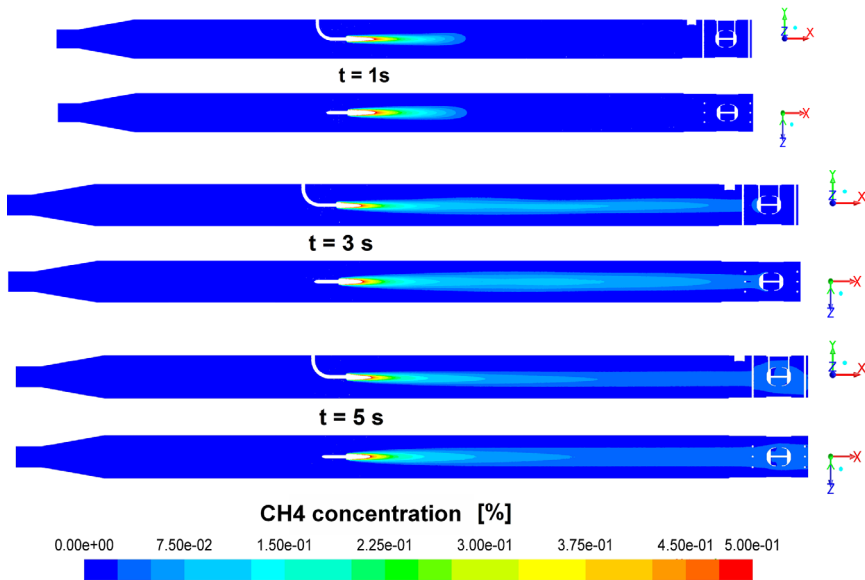


Fig. 16. Methane propagation in the station before opening of the valve – the distribution of the methane volume in both vertical and horizontal cross-sections along the station axis

concentration on the methane sensor filter surface was about 0.81% (Fig. 17). As a result of the simulation, a considerably lower methane concentration value was observed around the sensor than that recorded. The real methane stream was likely less dispersed.

### 8. Flow at the steady inflow

No significant fluctuations of the concentration field at the steady inflow conditions were found in assumed turbulence model (Figs. 18, 19).

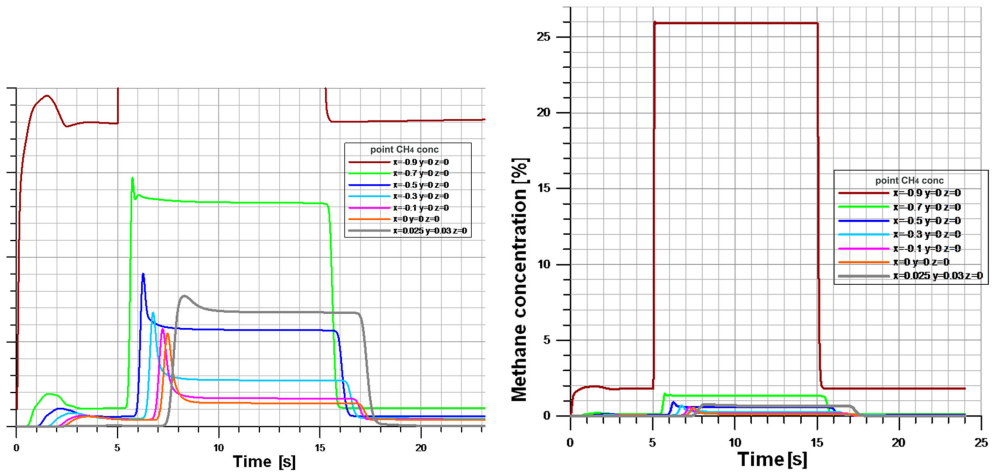


Fig. 17. Concentration changes with time for the virtual sensors before, during, and after feeding the methane and air mixture

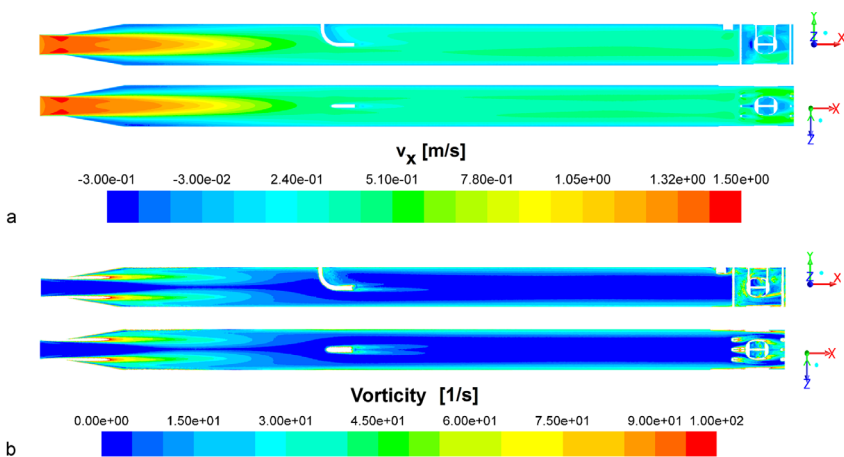


Fig. 18. Velocity field during the methane inflow – the component parallel to the axis.  
 b) Vorticity distribution from 0 up to 100 1/s, distributions in both vertical and horizontal cross-sections along the station axis

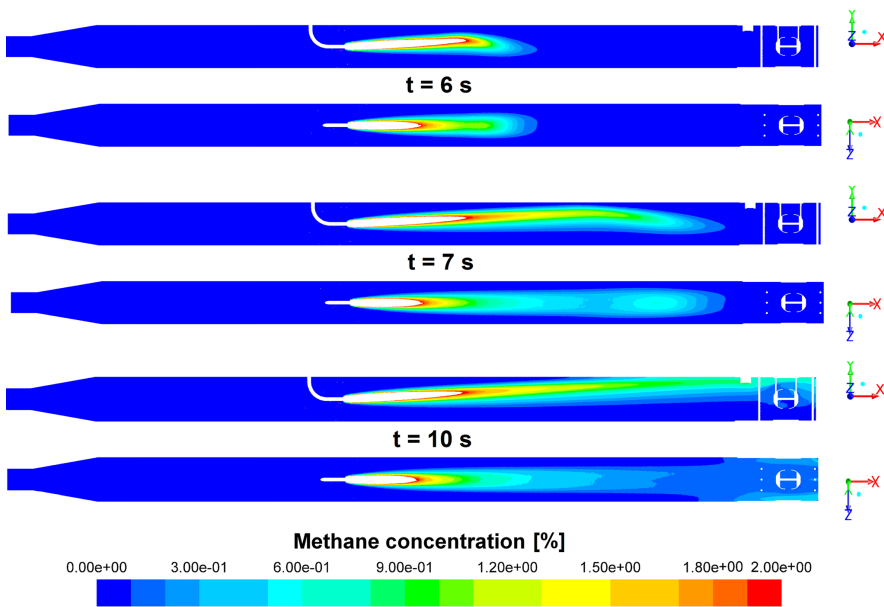


Fig. 19. The methane propagation after opening the valve – the distributions of the methane volume shares in both vertical and horizontal cross-sections along the station axis for the selected moments

### 9. The process of the removal of methane after the cut off of the mixture inflow

After 10 seconds of the inflow simulation, the methane inflow was gradually limited within 0,05 s. The calculations were carried on for 9 seconds. After about 5 seconds the concentration field has returned to the state from before the opening of the valve (Fig. 20).

### 10. Summary

The research carried out reveals a number of interesting results by recording methane velocities and concentrations with the anemometer vane sensor and pellistor sensor incorporated in the methane anemometer. These measurements were possible due to construction of an appropriate measurement station. The introduction of the methane stream into the air stream allowed approximation of the heterogeneous distribution of the methane concentration field in the methane anemometer measurement area. The variable stream velocity demonstrated a phase shift between the recordings of both sensors due to their different dynamic properties. This observed phase shift may cause measurement errors in non-mixed streams and/or varying velocity. The numerical simulations carried out did not fully illustrate the real flow phenomena. The methane concentration determined in the simulation was lower than that recorded by the sensor. This means that the real methane stream was less dispersed. The simulations provide a rough image of flow phenomena inside the test stand. Further studies might be aimed at refining the modeling to improve accuracy

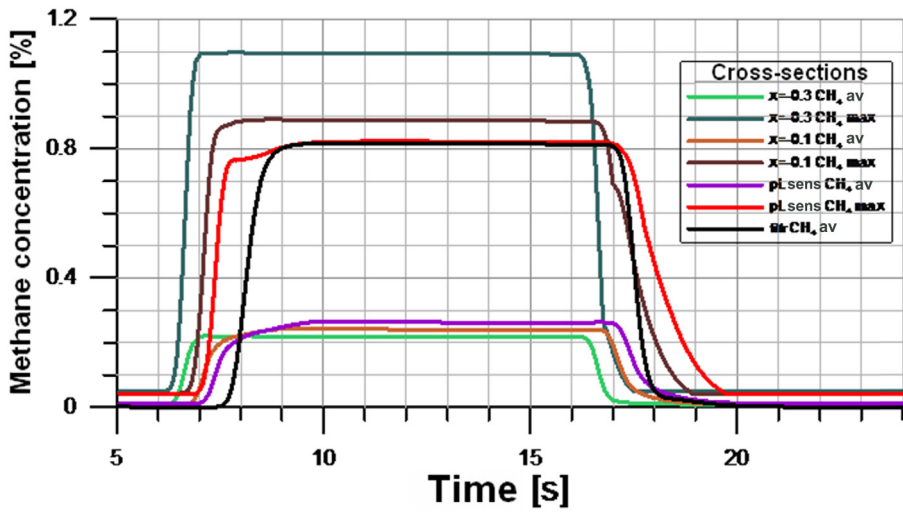


Fig. 20. The courses of the maximum and average concentrations for the selected station cross-sections

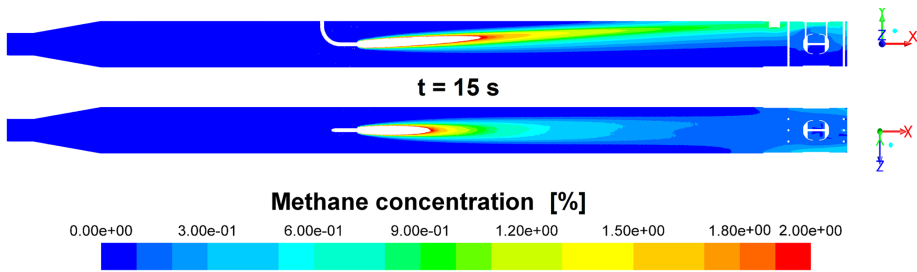


Fig. 21. Concentration distributions in both vertical and horizontal cross-sections

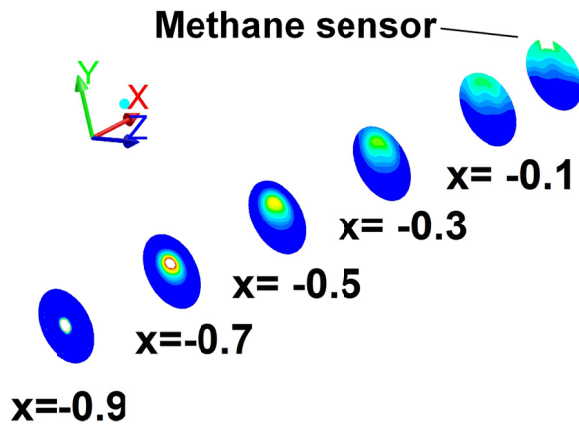


Fig. 22. The concentration distribution for the selected cross-sections

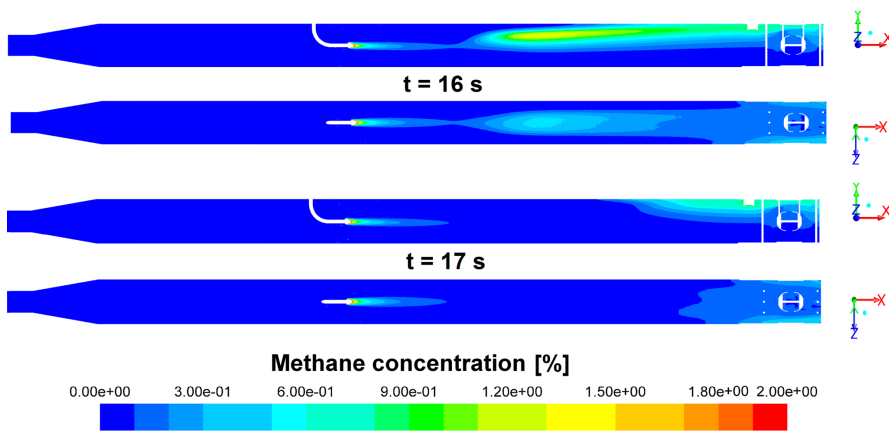


Fig. 23. Removal of methane after closing the valve – distributions of the methane volume shares in both vertical and horizontal cross-sections for the selected moments

and reproducing the unsteady flow experiments. Future research should address the dynamics of both sensors and *in-situ* experiments should be carried out to develop additional metrological procedures (calibration in the heading cross-section) in order to allow the instrument to determine the methane volume stream. In the present form, the methane anemometer can be used for the local measurement of methane velocity and concentration, and also provide an air flow velocity control in the area of the measuring chamber inlet.

## References

- ANSYS [2015] Fluent User Manual, Ansys Inc.
- Bogacz R., 2002. *Model matematyczny dyfuzji metanu przez osłonę ognioszczelną czujnika pellistorowego*. Zeszyty Naukowe. Elektryka / Politechnika Śląska, zeszyt 181. [Mathematical model of the methane diffusion through the flame-proof housing of pellistor sensor].
- Bogacz R., Krupanek B., 2014. *Kilka słów o błędzie dynamicznym czujnika pellistorowego w osłonie ognioszczelnej*. Przegląd Elektrotechniczny, R. 90, NR 11. [Several words on the dynamic error of the pellistor sensor in a flame-proof housing.].
- Bogacz R., Krupanek B., 2016. *Korekcja błędów dynamicznych czujnika pellistorowego w osłonie ognioszczelnej realizowana w sposób programowy*. Przegląd Elektrotechniczny, R. 92, NR 5. [Correction of the dynamic errors of pellistor sensor in the flame-proof housing implemented in a programmable way.].
- Janus J., Krawczyk J., Kruczkowski J., 2013. *Nowe rozwiązania urządzeń do pomiaru pól prędkości i rozkładów stężenia metanu oraz wyniki badań porównawczych*. Prace Instytutu Mechaniki Górotworu PAN. [New solutions for the devices intended for the measurements of the velocity fields and methane concentration distributions, and the results of comparative investigations.].
- Kruczkowski J., 2013a. *Rozkłady stężeń metanu w wyrobiskach przyścianowych. Zagrożenia aerologiczne w kopalniach węgla kamiennego – profilaktyka, zwalczanie, modelowanie, monitoring*. Główny Instytut Górnictwa. Katowice. [Distributions of the methane concentrations in by-longwall headings. Aerological hazards in hard coal mines – prevention, combating, modelling, monitoring.].
- Kruczkowski J., 2013b. *Wyznaczanie metanowości wentylacyjnej przy pomocy nowej techniki pomiarowej*. Materiały 7 Szkoły Aerologii Górniczej. Politechnika Śląska. Wydział Górnictwa i Geologii. Instytut Eksploatacji Złóż. Gli-



- wice. [Determination of the methane concentration in the ventilation air by means of a new measurement technique. Materials of the 7<sup>th</sup> Aerology Mining School.].
- Kruczkowski J., Ostrogórski P., 2013. *Urządzenie do pomiaru prędkości przepływu powietrza i stężenia metanu w wyrobisku kopalni*. Prace Instytutu Mechaniki Górniczej PAN. [Instrument for the measurement of the air flow velocity and methane concentration in a mine heading.]
- Kruczkowski J., Ostrogórski P., 2015. *Metanoanemometr SOM 2303. Nowoczesne metody zwalczania zagrożeń aerologicznych w podziemnych wyrobiskach górniczych*. Główny Instytut Górnictwa, Katowice. [SOM 2303 Methane anemometer. Modern methods of combating aerological hazards in underground mining headings.].
- Skotniczny P., 2014. *Stany przejściowe w przepływie mieszaniny powietrzno-metanowej na wylocie ze ściany wywołane nagłym wypływem metanu*. Archives of Mining Science, Vol. 59, Iss. 4. [Transient states in the flow of the air-methane mixture at the outlet from longwall triggered off by an abrupt methane outflow.].
- Wasilewski St., Araszczyk D., Jakubów A., 2015. *Wyznaczenie współczynnika korekcji między automatycznym pomiarem prędkości powietrza anemometrem stacjonarnym w systemie gazometrii automatycznej, a uśrednioną prędkością mierzoną anemometrem ręcznym. Nowoczesne metody zwalczania zagrożeń aerologicznych w podziemnych wyrobiskach górniczych*. Główny Instytut Górnictwa, Katowice. [Determination of the correction coefficient between the automatic air velocity measurement by means of the stationary anemometer in the system of automatic gasometry and the averaged velocity measured with hand-held anemometer. Modern methods of combating aerological hazards in underground mining headings.].